PHILOSOPHICAL TRANSACTIONS OF THE ROYAL SOCIETY A MATHEMATICAL, PHYSICAL & ENGINEERING SCIENCES

Axisymmetric and Non-Axisymmetric Flows of a Non-Newtonian Fluid between Coaxial Rotating Discs

I. Crewther, R. R. Huilgol and R. Jozsa

Phil. Trans. R. Soc. Lond. A 1991 **337**, 467-495
doi: 10.1098/rsta.1991.0134

Axisymmetric and non-axisymmetric flows of a non-newtonian fluid between coaxial rotating discs

By I. Crewther[1], R. R. Huilgol[2] and R. Jozsa[3]

[1] *Department of Physics and Mathematical Physics, University of Adelaide, Adelaide, South Australia 5000, Australia*

[2] *School of Information Science and Technology, Flinders University of South Australia, GPO Box 2100, Adelaide, South Australia 5001, Australia*

[3] *Department of Mathematics, Victoria University of Technology, GPO Box 2476V, Melbourne, Victoria 3001, Australia*

Contents

The axisymmetric and non-axisymmetric motions of a viscoelastic fluid driven by the steady rotations of a pair of coaxial, parallel discs, each of infinite extent, are studied analytically and numerically. The constitutive equation and the equations of motion depend altogether on four parameters and the numerical scheme used is robust and is capable of discovering regular and limit point bifurcations as well as folds arising from the changes in the values of the parameters.

First and foremost, the work reported here is an exhaustive collection of old and new results in the above flow problem, including the stability of the axisymmetric flows. Non-existence of bifurcations from the rigid body motion and their appearance from the torsional flow and other flows are found under a variety of conditions, extending from the newtonian to the non-newtonian fluid behaviour. Secondly, the

Phil. Trans. R. Soc. Lond. A (1991) **337**, 467–495
Printed in Great Britain

use of a scaling lemma permits the determination of the solutions to the problem over the entire range of parameters from the known solutions obtained for a finite range of the parameters. Thirdly, the type of non-axisymmetric flows likely to occur in the two-disc problem are determined numerically and they show that slip-layers may exist in the flow regime. These findings seem to confirm the experimental observations in the coaxial flow of a non-newtonian fluid.

1. Introduction

Nearly 70 years ago, von Kármán (1921) showed that the problem of finding the non-steady radial, azimuthal and axial velocities in an incompressible newtonian fluid undergoing an axisymmetric motion induced by the rotation of an infinitely wide disc could be reduced to finding the solution of a pair of nonlinear, coupled ordinary differential equations. Thirty years later, Batchelor (1951) considered the same problem when the fluid is confined between two parallel discs, each infinitely wide, and rotating about a common axis at speeds which could be different from one another. In the three decades and more since Batchelor's paper, much work has been done on these problems, both on the questions of existence and multiplicities of solutions and the numerical techniques of generating them. A survey of the analytical aspects is given by Parter (1982), while the theses by Szeto (1978) and Fier (1984) contain a great deal of material about the numerical work done on the axisymmetric two-disc problem.

As far as viscoelastic fluids are concerned, Phan-Thien (1983*a*) was the first to demonstrate that the solution of the time-dependent flow between rotating discs for a Maxwell fluid could be reduced to solving a system of coupled ordinary differential equations, consisting of the equations of motion and the constitutive equations. Subsequently, Phan-Thien (1983*b*) showed that the same situation arises with the Oldroyd-B fluid (Oldroyd 1950), which includes the newtonian and the Maxwell fluids as special cases.

Next, Huilgol & Keller (1985) laid the groundwork for finding the multiple solutions to the axisymmetric problem of the *steady flow* between rotating discs of an Oldroyd-B fluid. In particular, they showed by a *scaling lemma* that to examine the entire solution set it was sufficient to find the solutions for a restricted range of the angular velocity ratio of the top disc to that of the bottom one; see below for a precise statement. Unfortunately, their numerical scheme had some drawbacks and these were corrected by Walsh (1986, 1987), who converted the non-homogeneous boundary conditions on the stresses into homogeneous ones by a set of transformations of the constitutive equations and obtained a stable numerical scheme. In addition, Walsh was the first to show that bifurcations from a steady torsional flow occur; he established this by analytical means and verified that his numerical scheme agreed with the theoretical predictions. On the other hand, his scaling parameter did not enable him to study bifurcations from the rigid body motion, while our procedure does. See §2 below.

Now, Walsh's work (1987) was mainly concerned with axisymmetric flows of a Maxwell fluid. The extension to the Oldroyd-B fluid was first made by Crewther & Huilgol (1988). It has been vastly extended in the research reported here and, independently, by Ji *et al.* (1990). In our work, in Part A, we exhibit many examples of axisymmetric steady velocity fields for varying values of the four physical

parameters: the Reynolds number R, the angular velocity γ of the top disc assuming that the bottom disc has an angular velocity of unity, the relaxation time λ and the retardation time β. In addition, the bifurcation of solutions is discussed from both the analytical and the numerical perspectives. A similar set of objectives have been met by Ji *et al.* (1990) in their work. However, their work does not discuss the linearized stability of the flows they consider.

The first to do so systematically was Walsh (1986, 1987) who considered the linearized stability of steady, axisymmetric flows by resorting yet again to transformations of the constitutive equations. Using the latter, he obtained the analytical criterion for the linearized stability of a torsional flow and verified that his own condition for bifurcation from the steady torsional flow and Phan-Thien's (1983*b*) criterion for its stability were identical. In this paper, we use a set of transformations which are different from those of Walsh and having obtained by analytical means a condition for the stability of a torsional flow, we verify that our numerical scheme is also in agreement with it. Proceeding further, we examine the linearized stability of other flows by numerical techniques. This work places our research apart from that of Ji *et al.* (1990).

We now turn to steady non-axisymmetric motions in the above two-disc configuration. As far as newtonian fluids are concerned, Berker (1979) was the first to show that such solutions exist; he dealt with the case when the two discs were rotating with the same angular velocity. Next, Parter & Rajagopal (1984) examined the situation when the angular velocities were unequal; some numerical results for newtonian fluids were also published by Lai *et al.* (1984).

Turning to viscoelastic fluids, we find that Huilgol & Rajagopal (1987) were the first to show that in the Oldroyd-B fluid, non-axisymmetric motions occur. The important point about the non-axisymmetric motions in the newtonian and Oldroyd-B fluid is that these extra flow components are determined by the combined effects of the axisymmetric velocity field and the pressure gradient in the plane orthogonal to the axis of rotation.

In this paper, in Part B, we exhibit many examples of the non-axisymmetric steady velocity fields for varying values of the four physical parameters mentioned above. Our work is an extension of the earlier one reported by Crewther & Huilgol (1988). We remark in passing that the work by Ji *et al.* (1990) does not discuss any non-axisymmetric flows.

We note that Rajagopal (1991) has also prepared a review of the two-disc problem for newtonian and non-newtonian fluids. The aims of the present work and his are different for we are interested in exploring in detail the behaviour of a particular fluid, whereas he has surveyed the problem at a general level. In sum, it is believed that the present paper provides the most comprehensive picture of the flows of the Oldroyd-B fluid in the two-disc problem.

We now comment on why there is no mention of loss of hyperbolicity in the present work. To explain this, consider the chapter 11 of the recent book by Joseph (1990), where he has collected together the previous results by himself and his collaborators. He examines the behaviour of the Maxwell model in the axisymmetric flow between coaxial discs when the angular velocity ratio γ does not equal 1, i.e. when the discs rotate at different speeds. Joseph is concerned with the situation when the basic flow is such that there is a loss of hyperbolicity and hence the equations for the stress functions and the equations of motion in §3 below, with $\beta = 0$, lead to ill-posed problems. The loss of evolutionarity means that small changes in initial data lead to

PHILOSOPHICAL TRANSACTIONS OF THE ROYAL SOCIETY A MATHEMATICAL, PHYSICAL & ENGINEERING SCIENCES

large changes in the stresses or the velocity field. Our numerical results for the Oldroyd-B fluid, the main concern of the present research, show that as far as the velocity fields are concerned the problem is well posed on primary branches, a topic of concern to Joseph (1990). We are unable to say whether the problem is ill posed or not on other sheets. Of course, if we were to look at the Rayleigh problem (Tanner 1962) for the Oldroyd-B fluid for guidance on this matter, we find that the Maxwell model permits the sudden jump in the boundary velocity to propagate as a wave (of decreasing amplitude) whereas the Oldroyd-B fluid behaves like a newtonian fluid in the way the velocity disturbance is diffused. It seems to us therefore that loss of hyperbolicity has implications for the Maxwell fluid and not the Oldroyd-B fluid, and hence this question has not been investigated in the present paper.

2. The constitutive equation

In direct notation, the constitutive equation for the extra stress tensor $\hat{\boldsymbol{S}}$ in an incompressible Oldroyd-B fluid (Oldroyd 1950) is described by

$$\hat{\boldsymbol{S}}+\Lambda_1(\dot{\hat{\boldsymbol{S}}}-\hat{\boldsymbol{L}}\hat{\boldsymbol{S}}-\hat{\boldsymbol{S}}\hat{\boldsymbol{L}}^{\mathrm{T}})=\eta_0[\hat{\boldsymbol{A}}_1+\Lambda_2(\dot{\hat{\boldsymbol{A}}}_1-\hat{\boldsymbol{L}}\hat{\boldsymbol{A}}_1-\hat{\boldsymbol{A}}_1\hat{\boldsymbol{L}}^{\mathrm{T}})], \tag{2.1}$$

where $\hat{\boldsymbol{L}}$ is the velocity gradient corresponding to the velocity field $\hat{\boldsymbol{v}}$, $\hat{\boldsymbol{A}}_1$ is the first Rivlin–Ericksen tensor (Rivlin & Ericksen 1955), the superscript T denotes the transpose, with the three constants η_0, Λ_1 and Λ_2 being the viscosity, the relaxation time and the retardation time respectively. As is customary, it is assumed that $0 \leqslant \Lambda_2 \leqslant \Lambda_1$. In addition, the superposed dot denotes the material derivative, i.e.

$$\dot{\hat{\boldsymbol{A}}}_1=\partial\hat{\boldsymbol{A}}_1/\partial t+\nabla\hat{\boldsymbol{A}}_1\cdot\hat{\boldsymbol{v}}, \tag{2.2}$$

where the partial derivative is with respect to time t and ∇ is the spatial gradient operator.

Since we concentrate on the two-disc flow in this paper, let it be assumed that the lower disc rotates with a constant angular velocity Ω_0. Using this, we can scale the angular velocity Ω_1 of the upper disc and the other quantities as follows:

$$\left.\begin{gathered}\Omega_1=\gamma\Omega_0, \quad -\infty<\gamma<\infty,\\ \hat{\boldsymbol{v}}=\Omega_0\boldsymbol{v}, \quad \hat{\boldsymbol{S}}=\eta_0\Omega_0\boldsymbol{S}, \quad \lambda=\Omega_0\Lambda_1,\\ \beta=\Lambda_2/\Lambda_1, \quad 0\leqslant\beta\leqslant 1.\end{gathered}\right\} \tag{2.3}$$

With the above scaling the constitutive equation (2.1) now takes the form

$$\boldsymbol{S}+\lambda(\dot{\boldsymbol{S}}-\boldsymbol{L}\boldsymbol{S}-\boldsymbol{S}\boldsymbol{L}^{\mathrm{T}})=\boldsymbol{A}_1+\lambda\beta(\dot{\boldsymbol{A}}_1-\boldsymbol{L}\boldsymbol{A}_1-\boldsymbol{A}_1\boldsymbol{L}^{\mathrm{T}}). \tag{2.4}$$

In (2.4), $\boldsymbol{L}$ is the velocity gradient corresponding to $\boldsymbol{v}$ and $\boldsymbol{A}_1$ is calculated from $\boldsymbol{L}$. For later use we note that the newtonian limit can be obtained from (2.4) in two ways: either by setting $\beta=1$ with λ arbitrary, or by setting $\lambda=0$ and leaving β arbitrary. Additionally, the Maxwell model is the consequence of setting $\beta=0$ and $\lambda\neq 0$.

We remark that Phan-Thien (1983*a*, *b*) as well as Walsh (1986, 1987) have both used a different scaling parameter than the γ used here. Because they take the parameter to be equal to $\Omega_0/(\Omega_1-\Omega_0)$, the case of rigid body motions when the two angular velocities are equal becomes a singular point in the governing equations and Walsh (1986, 1987) is thus unable to discuss bifurcations from the rigid body motion.

PART A. AXISYMMETRIC MOTIONS

The plan of this part is as follows. In §3, we discuss the kinematics of steady, axisymmetric flows and the differential equations satisfied by the stress components, the transformed stresses and the equations of motion in terms of the latter. In §4, we recall the two known solutions: the rigid body motion and the torsional flow. Next, §5 is to establish that there are no bifurcations from the rigid body motion and to prove, following Walsh (1986, 1987), that there are bifurcations from the torsional flow. In §6, we discuss many examples of bifurcating flows from the torsional flow and secondary bifurcations from the primary ones, using numerical techniques. The effects of the Reynolds number R, the angular velocity ratio γ, the parameters λ and β are described in detail. In §7, we turn to non-steady flows and list the differential equations satisfied by the stresses and the transformed stresses, and the equations of motion again in terms of the latter. The §8 is devoted to the analytical aspects of the linearized stability of axisymmetric flows and a detailed examination of the stability of the torsional flow. In §9, we study the stability of some of the flows in §6 by computation. Thus Part A presents a fairly full picture of the steady flows, along with their linearized stabilities, of an Oldroyd-B fluid in the two-disc problem.

3. Steady axisymmetric flow equations

Assuming that the two infinitely wide, coaxial parallel discs are a distance d apart, we can non-dimensionalize the radial and axial coordinates $(\hat{r}, \hat{z})$ so that

$$\hat{r} = rd, \quad \hat{z} = zd. \tag{3.1}$$

We can now write the physical components of the velocity vector $\boldsymbol{v}$ as follows:

$$(v\langle r\rangle, v\langle\theta\rangle, v\langle z\rangle) = (rF', rG, -2F), \tag{3.2}$$

where F and G are unknown functions of z and the prime denotes differentiation with respect to z in (3.2) and in the sequel throughout. Using the adherence conditions at $z = 0$ (the bottom disc), and at $z = 1$ (the top disc), one finds that the boundary conditions on F and G are:

$$\left.\begin{aligned} F(0) = 0, \quad F(1) = 0, \quad G(0) = 1, \\ F'(0) = 0, \quad F'(1) = 0, \quad G(1) = \gamma. \end{aligned}\right\} \tag{3.3}$$

If the velocity field given by (3.2) is used in the constitutive equation (2.4), it can be shown (Phan-Thien 1983*b*; Huilgol & Keller 1985) that the stresses are given by the following set of equations:

$$\left.\begin{aligned} S\langle rr\rangle &= S_{10} + r^2 S_{11}, & S\langle\theta\theta\rangle &= S_{20} + r^2 S_{22}, \\ S\langle r\theta\rangle &= r^2 S_{12}, & S\langle\theta z\rangle &= r S_{23}, \\ S\langle rz\rangle &= r S_{13}, & S\langle zz\rangle &= S_{30}, \end{aligned}\right\} \tag{3.4}$$

where $S_{10}, S_{11}, \ldots, S_{30}$ are all functions of z. A fairly routine calculation shows that the above functions meet a system of ordinary differential equations (Phan-Thien 1983*b*; Huilgol & Keller 1985).

From these equations, it is obvious that the constitutive equations satisfied by S_{10} and S_{20} are identical. We shall assume therefore that these two functions are, in fact, *equal*. This equality is also necessary if the equations of motion are to be solvable;

for without this equality, the term $(S\langle rr\rangle - S\langle\theta\theta\rangle)/r$ in the r-component of the equations of motion makes them incompatible with one another. This point is discussed more fully by Huilgol & Keller (1985). A second bonus in assuming the equality of S_{10} and S_{20} lies in the fact that one can ignore these two functions for the rest of this Part A, as far as the analytical or numerical treatment of the problem is concerned. With this understanding, we proceed to discuss the remaining six functions.

As Walsh (1986, 1987) has pointed out in connection with his set of stress components, the remaining functions $S_{11}, \ldots, S_{30}$ introduce numerical complications because they require the values of F'' and G' on the boundaries $z = 0$ and $z = 1$. In particular, the troublesome ones are S_{11}, S_{12}, S_{13}, S_{22} and S_{23}. Now, because the derivatives $S'_{11}, \ldots, S'_{30}$ appear as multiples of F and also because $F(0) = F(1) = 0$, one can transform the functions $S_{11}, \ldots, S_{30}$ so that the new functions $T_{11}, \ldots, T_{30}$ will be zero on $z = 0$ and on $z = 1$. Thus, following Walsh (1987), we define the new functions as follows:

$$\left.\begin{aligned} T_{11} &= S_{11} - 2\lambda(1-\beta)F''^2, & T_{22} &= S_{22} - 2\lambda(1-\beta)G'^2, \\ T_{12} &= S_{12} - 2\lambda(1-\beta)F''G', & T_{23} &= S_{23} - G', \\ T_{13} &= S_{13} - F'', & T_{30} &= S_{30} + 4F'. \end{aligned}\right\} \tag{3.5}$$

It now follows that the above transformed stress functions $T_{11}, \ldots, T_{30}$ obey the following system of differential equations:

$$\left.\begin{aligned} T_{11} - 2\lambda[F(T'_{11} + 4\lambda(1-\beta)F''F''') + F''T_{13}] &= 0, \\ T_{12} - \lambda[2F(T'_{12} + 2\lambda(1-\beta)(F'''G' + F''G'')) + G'T_{13} + F''T_{23}\} &= 0, \\ T_{13} - \lambda[2FT'_{13} - 2F'T_{13} + F''T_{30} - 2(1-\beta)(FF''' - 3F'F'')] &= 0, \\ T_{22} - 2\lambda[F(T'_{22} + 4\lambda(1-\beta)G'G'') + G'T_{23}] &= 0, \\ T_{23} - \lambda[2FT'_{23} - 2F'T_{23} + G'T_{30} + 2(1-\beta)(FG'' - 3F'G')] &= 0, \\ T_{30} - 2\lambda[FT'_{30} - 2F'T_{30} - 4(1-\beta)(2F'^2 - FF'')] &= 0. \end{aligned}\right\} \tag{3.6}$$

Unlike the situation that occurs with systems of differential equations, the above set is valid on the end points $z = 0$ and $z = 1$ because the differential equations correspond to *constitutive equations* (Huilgol & Keller 1985). It is then very easily verified that $T_{11}, \ldots, T_{30}$ are all zero on $z = 0$ and $z = 1$.

When the pressure term is eliminated from the r and z equations, the equations of motion lead to the following:

$$3T'_{11} - T'_{22} + T''_{13} + 4\lambda(1-\beta)(3F''F''' - G'G'') + F^{\mathrm{iv}} + 2R(FF''' + GG') = 0, \tag{3.7}$$

where the Reynolds number R is defined through:

$$R = \rho\Omega_0 d^2/\eta_0, \tag{3.8}$$

and ρ is the density of the fluid. The equation of motion in the θ-direction gives the second equation:

$$4T_{12} + T'_{23} + 8\lambda(1-\beta)F''G' + G'' - 2R(F'G - FG') = 0, \tag{3.9}$$

when it is realized that the pressure term is independent of the θ coordinate.

In sum, the relevant equations for steady, axisymmetric motions of an Oldroyd-B fluid in the two-disc problem are given by (3.6)–(3.9), with the boundary conditions (3.3) for F, F' and G, and zero boundary conditions for the six functions $T_{11}, \ldots, T_{30}$ appearing in (3.6).

4. Two basic solutions

We now recall the nature of the two steady axisymmetric solutions to the above set of equations. The first is the rigid body motion and the second is the torsional flow.

(*a*) *Rigid body motion*

In this situation, in the boundary conditions (3.3), the parameter $\gamma = 1$ because the top and bottom discs rotate with the same angular velocity. It follows therefore that the entire body of the fluid can rotate as a rigid body, or

$$F(z) \equiv 0, \quad G(z) \equiv 1, \tag{4.1}$$

for all values of R (i.e. inertia is included), λ and β. From (4.1) we see that all the stress functions $T_{11}, \ldots, T_{30}$ in (3.6) are zero.

(*b*) *Torsional flow*

Here, the fluid body undergoes a shearing flow with the angular velocity changing from 1 at the bottom disc to γ at the top. Again, there are no radial and axial velocity components. Thus

$$F(z) \equiv 0, \quad G(z) = 1 + (\gamma - 1)\, z. \tag{4.2}$$

This solution is true for all values of λ and β. However, the Reynolds number $R = 0$, that is inertia must be ignored. Moreover, all the stress functions $T_{11}, \ldots, T_{30}$ are zero; note, however, that the original stresses are not all zero. In fact, from (3.5) it follows that the non-zero stresses are

$$\left.\begin{aligned} S_{22} &= 2\lambda(1-\beta)\,(\gamma-1)^2, \\ S_{23} &= \gamma - 1. \end{aligned}\right\} \tag{4.3}$$

5. Bifurcations from the basic solutions

To study bifurcations from a known solution, we assume that each of the functions F, G, $T_{11}, \ldots, T_{30}$ can be represented as:

$$U(z;\epsilon) = U^0(z) + \epsilon u(z) + O(\epsilon^2), \tag{5.1}$$

where $U(\cdot)$ stands for any of the eight functions F, G, $T_{11}, \ldots, T_{30}$; $U^0(\cdot)$ denotes the value of each in the primary flow situation and $u(\cdot)$ is the first-order perturbation term. Thus in §5 we let $(f, g, t_{11}, \ldots, t_{30})$ stand for the perturbations in $(F, G, T_{11}, \ldots, T_{30})$ respectively.

Now, as far as the stress perturbations $t_{11}, \ldots, t_{30}$ are concerned, one can obtain those relevant to the torsional flow from (3.6) by using the flow (4.2) as the primary one. These stress perturbations can also be made pertinent to the rigid body motion simply by putting the parameter $\gamma = 1$ in the ensuing results. Because the functions F^0, $T^0_{11}, \ldots, T^0_{30}$ are all zero in the torsional flow, and

$$G^0(z) = 1 + (\gamma - 1)\, z, \tag{5.2}$$

it follows that the perturbation stress functions obey the following:

$$\left.\begin{aligned} t_{11} &= t_{12} = t_{30} = t_{13} = 0, \\ t_{22} &= -12\lambda^2(1-\beta)\,(\gamma-1)^2 f', \\ t_{23} &= -6\lambda(1-\beta)\,(\gamma-1) f', \end{aligned}\right\} \tag{5.3}$$

where f and g represent the respective perturbations of F and G. Of course, in deriving (5.3), all terms of order $O(\epsilon^2)$ have been ignored. Also, it must be noted that on the boundaries $z = 0$ and $z = 1$, the perturbations $f, f', g, t_{11}, \ldots, t_{30}$ are all zero.

(a) *Rigid body motion*

In this case, we known from (5.3) that $t_{22} = 0$ because $\gamma = 1$. Thus the equations of motion (3.7) and (3.9) lead to:

$$\left.\begin{aligned} f^{\mathrm{iv}} + 2Rg' &= 0, \\ g'' - 2Rf' &= 0. \end{aligned}\right\} \tag{5.4}$$

If we multiply the first equation by f, use the boundary conditions

$$f(0) = f(1) = 0, f'(0) = f'(1) = 0, \tag{5.5}$$

and integrate by parts, we find that

$$\int_0^1 f''^2 \, \mathrm{d}z + 2R \int_0^1 fg' \, \mathrm{d}z = 0. \tag{5.6}$$

Next, multiply the second equation in (5.4) by g, use the boundary conditions

$$g(0) = g(1) = 0, \tag{5.7}$$

and integrate by parts. We have

$$-\int_0^1 g'^2 \, \mathrm{d}z + 2R \int_0^1 fg' \, \mathrm{d}z = 0. \tag{5.8}$$

If we subtract (5.8) from (5.6) it is found that the two functions $f''(z)$ and $g'(z)$ are both identically zero on the interval $0 \leqslant z \leqslant 1$. Using the boundary conditions (5.5) and (5.7), it is trivial to prove that (Crewther & Huilgol 1988)

$$f(z) = 0, \quad g(z) = 0, \quad 0 \leqslant z \leqslant 1. \tag{5.9}$$

Hence we have shown that there are no bifurcations from the rigid body motion in the two-disc flow for the Oldroyd-B fluid (Crewther & Huilgol 1988). As remarked earlier, Walsh (1986, 1987) is unable to discuss the case of bifurcations from a rigid body motion because the scaling of the angular velocity has been done through the ratio $\Omega_0/(\Omega_1 - \Omega_0)$ and this becomes infinite in a rigid body motion. Parenthetically, we remark that our result shows that there are no bifurcations from the rigid body motion for a newtonian fluid either, although such a result was established earlier by Cerutti (1975) according to Parter (1982).

(b) *Torsional flow*

Turn now to the equations of motion (3.7) and (3.9), put $R = 0$ there, and use (5.2) and (5.3) to the effect that t_{11}, t_{12}, and t_{13} are all zero and that t_{22} and t_{23} are non-zero. It then follows that

$$f^{\mathrm{iv}} + 12\lambda^2(1-\beta)(\gamma-1)^2 f'' - 4\lambda(1-\beta)(\gamma-1)g'' = 0, \tag{5.10}$$

$$2\lambda(1-\beta)(\gamma-1)f'' + g'' = 0. \tag{5.11}$$

Eliminating g'' from the above equations, we find that (Walsh 1986, 1987)

$$f^{\mathrm{iv}} + 4\delta^2 f'' = 0, \tag{5.12}$$

where the parameter δ is given by

$$\delta^2 = \lambda^2(1-\beta)(\gamma-1)^2[3+2(1-\beta)]. \tag{5.13}$$

Using the boundary conditions (5.5) we find that the equation (5.12) has non-trivial solutions whenever δ satisfies the equation:

$$\delta \sin 2\delta + \cos 2\delta = 1. \tag{5.14}$$

This transcendental equation has two sets of solutions:

$$\left.\begin{aligned} \delta &= n\pi, \quad n = 0, 1, 2, \ldots, \\ \delta &= \tan \delta. \end{aligned}\right\} \tag{5.15}$$

We can disregard $n = 0$, for this leads to a trivial solution of (5.12). It is thus clear that (5.12) has an infinite number of bifurcating points and that each is *simple*. Without this knowledge, in the numerical scheme that Huilgol & Keller (1985) tried earlier attention was focused on finding simple bifurcation points only. It now turns out, due to the efforts of Walsh (1986, 1987), that this was indeed the right decision. Thus in the next §6 we find simple bifurcation points only and trace out the consequences of this assumption. It particular, it is clear that the parameter δ can be changed by varying any of the three parameters λ, β and γ. It is thus not surprising that the solution set for the two-disc problem has such a rich structure.

6. Numerical study of bifurcations from steady axisymmetric flows

Before we discuss the method adopted to find the bifurcating solutions from any known solution, we wish to point out that the angular velocity ratio parameter γ used here permits the following *Scaling Lemma* (Huilgol & Keller 1985) to be proved.

Scaling Lemma. *If the functions* $F, G, T_{11}, \ldots, T_{30}$ *of* z *in* $0 \leqslant z \leqslant 1$, *and the parameters* $R, \lambda, \beta, \gamma$ *solve the system of equations* (3.6), (3.7) *and* (3.9), *then the functions* $\tilde{F}, \tilde{G}, \tilde{T}_{11}, \ldots, \tilde{T}_{30}$ *of* ζ *in* $0 \leqslant \zeta \leqslant 1$ *and the parameters* $\tilde{R}, \tilde{\lambda}, \tilde{\beta}, \tilde{\gamma}$ *solve the problem under the transformations*:

$$\left.\begin{aligned} \zeta = 1-z, \quad \tilde{R} = |\gamma| R, \quad \tilde{\lambda} = \lambda|\gamma|, \quad \tilde{\beta} = \beta, \quad \tilde{\gamma} = 1/\gamma, \\ \tilde{F}(\zeta) = -F(z)/|\gamma|, \quad \tilde{G}(\zeta) = G(z)/\gamma, \\ \tilde{T}_{11} = T_{11}/|\gamma|, \quad \tilde{T}_{12} = T_{12}/\gamma, \\ \tilde{T}_{13} = -T_{13}/|\gamma|, \quad \tilde{T}_{22} = T_{22}/|\gamma|, \\ \tilde{T}_{23} = -T_{23}/\gamma, \quad \tilde{T}_{30} = T_{30}/|\gamma|. \end{aligned}\right\} \tag{6.1}$$

The above lemma, which is easily proved, shows that we need only consider γ in the strip $-1 \leqslant \gamma \leqslant 1$ to obtain solutions for γ in $-\infty < \gamma < \infty$. We remark that such a lemma is not provable under the scaling laws assumed by Phan-Thien (1983*a*, *b*) and Walsh (1986, 1987).

We now describe the numerical scheme adopted to solve the equations (3.6), (3.7) and (3.9). First of all, to use the programme of Fier (1984) and to compare our results with his, we convert the above three sets of equations into a second-order system. To this end, let us define a new variable H through

$$F'' = H. \tag{6.2}$$

Next, to minimize the band width in the computational scheme, we rewrite the full system as:

$$\left.\begin{aligned}
T_{11}-2\lambda[F(T'_{11}+4\lambda(1-\beta)HH')+HT_{13}] &= 0,\\
3T'_{11}-T'_{22}+T''_{13}+4\lambda(1-\beta)(3HH'-G'G'')+H''+2R(FH'+GG') &= 0,\\
T_{13}-\lambda[2FT'_{13}-2F'T_{13}+HT_{30}-2(1-\beta)(FH'-3F'H)] &= 0,\\
4T_{12}+T'_{23}+8\lambda(1-\beta)G'H+G''-2R(F'G-FG') &= 0,\\
T_{12}-\lambda[2F(T'_{12}+2\lambda(1-\beta)(G'H'+G''H))+G'T_{13}+HT_{23}] &= 0,\\
T_{22}-2\lambda[F(T'_{22}+4\lambda(1-\beta)G'G'')+G'T_{23}] &= 0,\\
F''-H &= 0,\\
T_{23}-\lambda[2FT'_{23}-2F'T_{23}+G'T_{30}+2(1-\beta)(FG''-3F'G')] &= 0,\\
T_{30}-2\lambda[FT'_{30}-2F'T_{30}-4(1-\beta)(2F'^2-FH)] &= 0.
\end{aligned}\right\} \tag{6.3}$$

The above system is of second order with nine equations and 18 *boundary conditions*, the six imposed ones on F, F' and G and the twelve *natural* ones on the stresses $T_{11}, \ldots, T_{30}$. To solve this system, we set up a mesh by dividing the interval $[-\frac{1}{2}\Delta z, 1+\frac{1}{2}\Delta z]$ into J equal subintervals, where $\Delta z = 1/(J-1)$. The discretized equations are obtained by making the following substitutions:

$$\left.\begin{aligned}
U_{9j+1} &= T_{11}, \quad U_{9j+2} = T_{13}, \quad U_{9j+3} = T_{12},\\
U_{9j+4} &= T_{22}, \quad U_{9j+5} = H, \quad U_{9j+6} = G,\\
U_{9j+7} &= F, \quad U_{9j+8} = T_{23}, \quad U_{9j+9} = T_{30},
\end{aligned}\right\} \quad j = 0, 1, \ldots, J. \tag{6.4}$$

Next, we write the difference equations about the end points of the subintervals and use the standard three-point formulae to approximate the first and second derivatives. We approximate the boundary conditions at $z = 0$ and $z = 1$ by using the mesh points $j = 0$, $j = 1$ and $j = J-1$, $j = J$ respectively with averages for function values and differences for the derivatives. That is, let V stand for any of the nine variables and number the mesh points j from 0 to J.

At the end point $z = 0$, one has

$$V(0) = \tfrac{1}{2}(V_0 + V_1), \quad V'(0) = (1/\Delta z)(V_1 - V_0), \tag{6.5}$$

where V_0 and V_1 stand for the values of V at the mesh points $j = 0$ and $j = 1$ respectively. A formula similar to (6.5) holds for $V(1)$ and $V'(1)$ at the end point $z = 1$. At an interior point z_j, we set

$$V(z_j) = V_j, \quad j = 1, \ldots, J-1. \tag{6.6}$$

Then,

$$\left.\begin{aligned}
V'_j &= (V_{j+1} - V_{j-1})/2\Delta z,\\
V''_j &= (V_{j+1} - 2V_j + V_{j-1})/\Delta z^2.
\end{aligned}\right\} \tag{6.7}$$

Using the above central difference formulae, we recast the system (6.3) into a set of algebraic equations which we denote by the operator equation

$$\boldsymbol{G}(\boldsymbol{U}, R, \gamma, \lambda, \beta) = \boldsymbol{0}. \tag{6.8}$$

In recent years, much work has been done on the solution of equations such as (6.8)

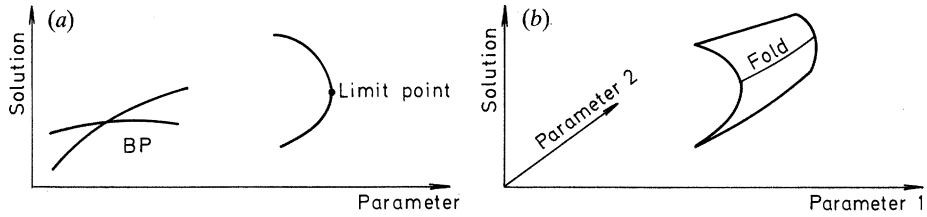

Figure 1. (*a*) Regular bifurcation point (BP) and limit point. (*b*) Limit point and a fold.

to find regular bifurcations, limit points, folds, etc. For a full description of the techniques, see Keller (1987). Here, we have illustrated some of these terms in figure 1*a* and *b*.

As mentioned earlier, we have used the program of Fier (1984) to solve the system (6.8). The reader's attention is drawn to the book by Keller (1987) and Fier's thesis, where the requisite mathematics is described fully. Briefly, the program of Fier depends on a number of subroutines which use the methods of regular and pseudo-arc-length continuations; methods to locate both regular bifurcating points and limit points; techniques to switch solutions at regular bifurcating points and to follow folds.

Consistency check. Because the program to solve (6.8) is rather large, it is necessary to devise a consistency check to ensure that the program functions correctly. Of course, the program must give the right answers for the rigid body motion (4.1) and the torsional flow (4.2). Unfortunately, these two do not provide a sufficiently good check because so many terms are zero. Hence we devised two continuation problems based on the fact that the newtonian solution can be obtained from the Oldroyd-B fluid solution through two limits: by setting $\lambda = 0$ and leaving β arbitrary, or by putting $\beta = 1$ and leaving λ arbitrary. The authors will supply the interested reader the full details of these calculations.

To check that the subroutines to discover the regular bifurcating points and the switching of solutions performed correctly, we chose to demonstrate that no bifurcation points arise from the rigid body motion and that those that emanate from the torsional flow meet (5.12) and (5.13).

Unfortunately, we were unable to devise any means of checking whether those subroutines concerned with limit points and fold continuations functioned accurately for the Oldroyd-B fluid, although these subroutines produced results in agreement with those results of Fier (1984) for the newtonian fluid, obtained by putting $\lambda = 0$ in the relevant equations.

By solving the discretized equations (6.8) and using $J = 49$ subintervals, we obtained, literally, hundreds of solutions. From this set, we have selected those that are interesting in themselves or those that could be compared with the work of Walsh (1986, 1987) or Ji *et al.* (1990). These are described below in six groups. In all of the six groups, we have depicted the variations from the torsional flow, i.e. $F(z)$ and

$$\Delta G(z) = G(z) - [1 + (\gamma - 1)\, z]. \tag{6.9}$$

Example Set I

In this set, we keep $\gamma = -0.5$, i.e. the top disc is set to rotate at half the speed of the bottom one in the opposite direction, and $\beta = 0.5$ fixed. Attention is now drawn to figures 2–6, where we have sketched the graphs of the functions F and ΔG.

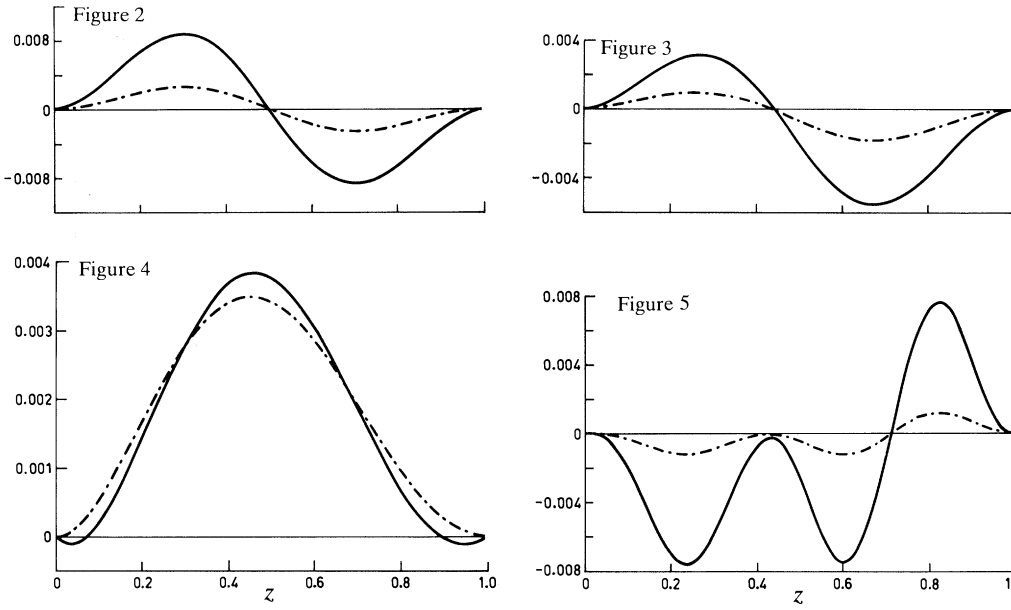

Figures 2–5. ——, ΔG; – – – –, F.

Figure 2. Solution on the first bifurcation branch off torsional flow. $R = 4.3 \times 10^{-13}$, $\lambda = 2.0$. See §6, Example set I for additional information regarding figures 2–6.

Figure 3. Solution at the first limit point obtained by changing $R = 0$ to $R = 0.24$ while keeping $\lambda = 2.0$ fixed.

Figure 4. Solution at $R = 0.99$ and $\lambda = 1.0$. Unable to generate non-axisymmetric flow for this one.

Figure 5. Solution at one more limit point with $R = 1.4$ and $\lambda = 3.9$.

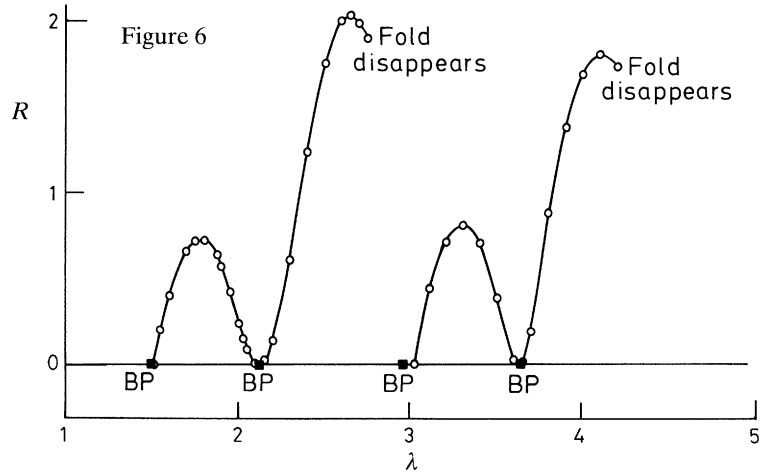

Figure 6. The folds in the $R\lambda$-plane. Here BP denotes a regular bifurcation point.

The procedure to generate this set is as follows: begin with the torsional flow solution using $R = 0$, $\gamma = -0.5$ and $\beta = 0.5$. Vary the parameter λ and use the relevant subroutines till the first bifurcation point is reached. From (5.13) and (5.15) we see that the first bifurcation point occurs when $\delta = \pi$, or when $\lambda = 1.481$. Follow

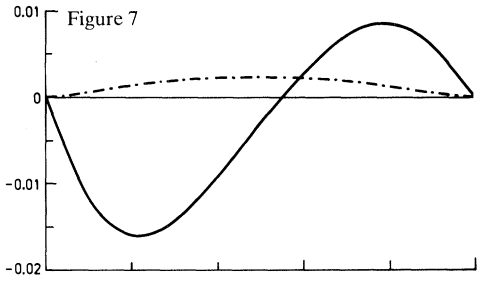

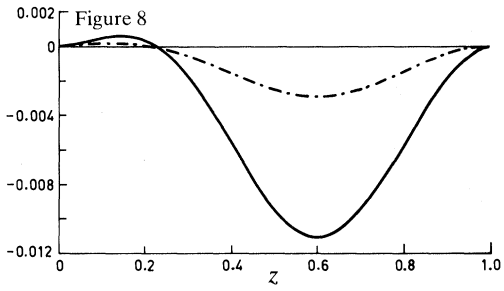

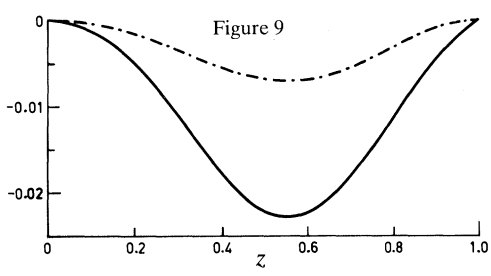

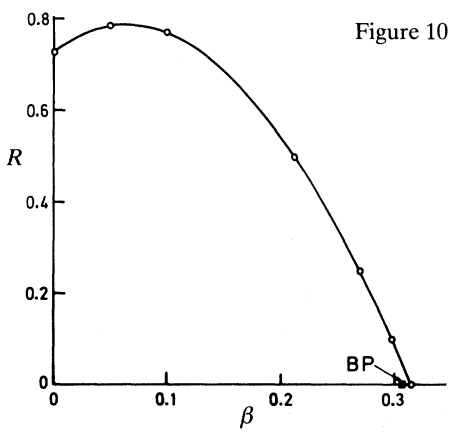

Figures 7–10. ——, ΔG; – – –, F.

Figure 7. Solution with $R = 50$ and $\beta = 0.98$. The flow pattern in an almost newtonian fluid. See §6, Example set II for more information regarding figures 8–10.

Figure 8. Solution at a limit point with $R = 0.73$ and $\beta = 0.0$. The flow pattern in a Maxwell fluid.

Figure 9. Solution at a limit point with $R = 0.1$ and $\beta = 0.3$.

Figure 10. The folds in the $R\beta$-plane. Again, BP denotes a regular bifurcation point.

the new path until the value of $\lambda = 2$. The solution so obtained is in figure 2. If we now keep three parameters fixed and change R from 0 to 0.24, we derive at a limit point and figure 3 illustrates the functions F and ΔG. It is clear that the symmetry of the solutions has disappeared in going from $R = 0$ to $R = 0.24$.

Proceeding in the fashion described above, we have obtained a variety of flow curves and these are illustrated in figures 3–5. In the last figure 6, the rich bifurcation structure is depicted by showing the bifurcation points and folds in the $R\lambda$-plane. It is found that when the folds in the $R\lambda$-plane disappear, the solution surface becomes smooth.

Example Set II

Here, we keep $\gamma = 0.5$ and $\lambda = 3.6$, which is a rather large value for the relaxation time, fixed and vary R and β. The value of $\beta = 0$ corresponds to the Maxwell fluid and that of $\beta = 1$ to that of the newtonian fluid. The results are drawn in figures 7–10, with the last one being that of the folds in the $R\beta$-plane.

PHILOSOPHICAL TRANSACTIONS OF THE ROYAL SOCIETY A MATHEMATICAL, PHYSICAL & ENGINEERING SCIENCES

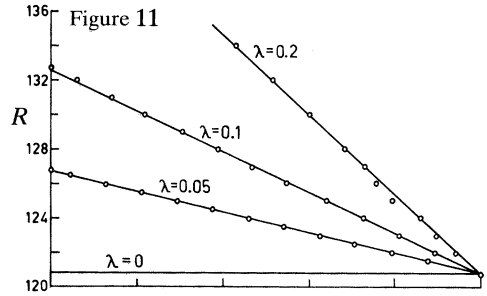

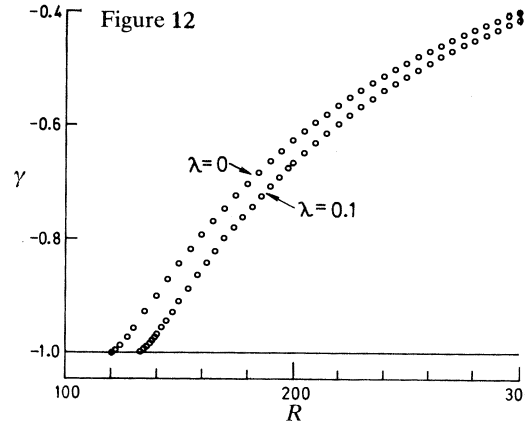

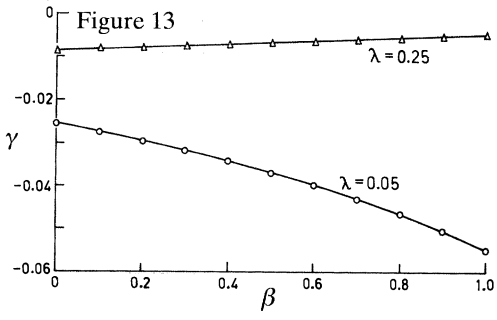

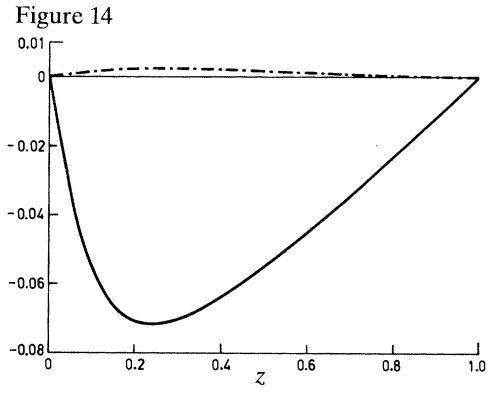

Figure 11. In Example Set III of §6, bifurcation points for $\gamma = -1$ while varying R from 120 to 138, β from 0 to 1 and λ from 0 to 0.2 are drawn.

Figure 12. In Example Set IV of §6, folds in the $R\gamma$-plane for the Maxwell fluid with $\beta = 0$ and λ varying from 0 to 0.1 are depicted.

Figure 13. In Example Set V of §6, folds in the $\beta\gamma$-plane with $R = 200$ and λ varying from 0.05 to 0.25 are drawn.

Figure 14. In Example Set VI of §6, solution at first limit point obtained with $R = 200$, $\beta = 0.5$, $\lambda = 0.05$ and $\gamma = -0.0055$. ——, ΔG; – – –, F.

Example Set III

Here, the computed bifurcation points when the three parameters R, λ and β are varied by keeping $\gamma = -1$ fixed are shown in figure 11.

Example Set IV

Here, in figure 12, we show the folds in the $R\gamma$-plane when the Maxwell model, i.e. $\beta = 0$, is examined.

Example Set V

Figure 13 depicts the folds in the $\beta\gamma$-plane when $R = 200$ and λ varying from $\lambda = 0.05$ to 0.25 for extremely small speeds (γ) of rotation of the top disc.

PHILOSOPHICAL TRANSACTIONS OF THE ROYAL SOCIETY A MATHEMATICAL, PHYSICAL & ENGINEERING SCIENCES

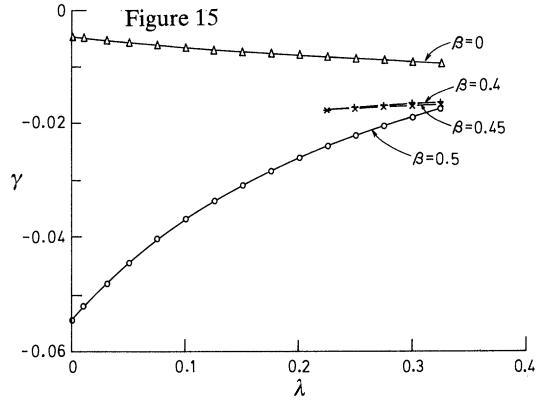

Figure 15. Folds in the $\gamma\lambda$- plane with $R = 200$ and β varying from 0 to 0.5.

Example Set VI

Suppose we begin with $R = 200$, $\beta = 0.5$, $\lambda = 0.05$ and $\gamma = 1$, i.e. when the fluid is undergoing a rigid body motion, and decrease the value of γ. Then the first limit point is obtained at the value of $\gamma = -0.0055$ and figure 14 shows this solution. The last figure 15 is that of the folds in the $\gamma\lambda$-plane with $R = 200$ as β varies from 0.0 to 0.05.

7. Non-steady axisymmetric flows

Here we assume that the velocity field is described in terms of two functions $F(z,t)$ and $G(z,t)$ and that the flow components are given by (cf. 3.2)):

$$(v\langle r\rangle, v\langle\theta\rangle, v\langle z\rangle) = (rF', rG, -2F), \tag{7.1}$$

where the prime denotes partial differentiation with respect to z. The boundary conditions on the functions are:

$$\left.\begin{aligned} F(0,t) = 0, \quad F(1,t) = 0, \quad G(0,t) = 1,\\ F'(0,t) = 0, \quad F'(1,t) = 0, \quad G(1,t) = \gamma. \end{aligned}\right\} \tag{7.2}$$

Given the velocity field (7.1), it can again be shown (Phan-Thien 1983*b*) that the stresses are given by the set of equations as written in (3.4) above, except that the eight functions $S_{10}, S_{11}, \ldots, S_{30}$ are now functions of z and t. For the sake of brevity, we omit the equations satisfied by the functions S_{10} and S_{20} and assume that these functions are equal. We now list the differential equations satisfied by the remaining six functions:

$$\left.\begin{aligned} S_{11} + \lambda(\dot{S}_{11} - 2FS'_{11} - 2F''S_{13}) &= -2\beta\lambda F''^2,\\ S_{12} + \lambda(\dot{S}_{12} - 2FS'_{12} - G'S_{13} - F''S_{23}) &= -2\beta\lambda F''G',\\ S_{13} + \lambda(\dot{S}_{13} - 2FS'_{13} + 2F'S_{13} - F''S_{30}) &= F'' + \beta\lambda(\dot{F}'' + 6F'F'' - 2FF'''),\\ S_{22} + \lambda(\dot{S}_{22} - 2FS'_{22} - 2G'S_{23}) &= -2\beta\lambda G'^2,\\ S_{23} + \lambda(\dot{S}_{23} - 2FS'_{23} + 2F'S_{23} - G'S_{30}) &= G' + \beta\lambda(\dot{G}' + 6F'G' - 2FG''),\\ S_{30} + \lambda(\dot{S}_{30} - 2FS'_{30} + 4F'S_{30}) &= -4F' - 4\beta\lambda(\dot{F}' - 2FF'' + 4F'^2). \end{aligned}\right\} \tag{7.3}$$

The equations of motion for the unsteady flow problem are given by:

$$\left.\begin{aligned} 3S'_{11} - S'_{22} + S''_{13} &= R(\dot{F}'' - 2FF''' - 2GG'),\\ 4S_{12} + S'_{23} &= R(\dot{G} + 2F'G - 2FG'). \end{aligned}\right\} \tag{7.4}$$

PHILOSOPHICAL TRANSACTIONS OF THE ROYAL SOCIETY A MATHEMATICAL, PHYSICAL & ENGINEERING SCIENCES

In the above set (7.3) and (7.4), the superposed dot denotes the partial derivative with respect to t, whereas the prime denotes the partial derivative with respect to z. In the steady flow situation, we followed Walsh (1986, 1987) and introduced a set of stress functions which vanished on the boundaries $z = 0$ and $z = 1$. Here, we introduce a new set of stress functions to facilitate the treatment of the linearized stability problem in §8. The basic idea behind the transformations is to have the time derivatives appearing in the simplest possible way in the constitutive equations and the equations of motion. Thus we combine the two time derivatives which appear in (2.4) and replace $\boldsymbol{S}$ by $\boldsymbol{W}$, which we define through:

$$\boldsymbol{S} = \boldsymbol{W} + \beta \boldsymbol{A}_1. \tag{7.5}$$

As a consequence, the following relations exist between the stress functions S_{ij} and the W_{ij}:

$$\left.\begin{aligned} S_{11} &= W_{11}, & S_{13} &= W_{13} + \beta F'', \\ S_{12} &= W_{12}, & S_{23} &= W_{23} + \beta G', \\ S_{22} &= W_{22}, & S_{30} &= W_{30} - 4\beta F'. \end{aligned}\right\} \tag{7.6}$$

Indeed, the above transformations have the effect of removing the time derivatives from the right side of the equations affecting S_{13}, S_{23}, and S_{30} in the list (7.3), as well as removing all the nonlinear terms from the right side of the constitutive equations for the S_{ij} in (7.3). In terms of the new stress functions W_{ij}, the constitutive equations are given by:

$$\left.\begin{aligned} W_{11} + \lambda(\dot{W}_{11} - 2FW'_{11} - 2F''W_{13}) &= 0, \\ W_{12} + \lambda(\dot{W}_{12} - 2FW'_{12} - G'W_{13} - F''W_{23}) &= 0, \\ W_{13} + \lambda(\dot{W}_{13} - 2FW'_{13} + 2F'W_{13} - F''W_{30}) &= (1-\beta)F'', \\ W_{22} + \lambda(\dot{W}_{22} - 2FW'_{22} - 2G'W_{23}) &= 0, \\ W_{23} + \lambda(\dot{W}_{23} - 2FW'_{23} + 2F'W_{23} - G'W_{30}) &= (1-\beta)G', \\ W_{30} + \lambda(\dot{W}_{30} - 2FW'_{30} + 4F'W_{30}) &= -4(1-\beta)F'. \end{aligned}\right\} \tag{7.7}$$

Next, the equations of motion are:

$$\left.\begin{aligned} \beta F^{\mathrm{iv}} + 3W'_{11} - W'_{22} + W''_{13} &= R(\dot{F}'' - 2FF''' - 2GG'), \\ \beta G'' + 4W_{12} + W'_{23} &= R(\dot{G} + 2F'G - 2FG'), \end{aligned}\right\} \tag{7.8}$$

For future use, we note the boundary values taken by the above six functions when the flow is *steady*. These values are:

$$\left.\begin{aligned} W_{11} &= 2\lambda(1-\beta)F''^2, & W_{22} &= 2\lambda(1-\beta)G'^2, \\ W_{12} &= 2\lambda(1-\beta)F''G', & W_{23} &= (1-\beta)G', \\ W_{13} &= (1-\beta)F'', & W_{30} &= 0. \end{aligned}\right\} \tag{7.9}$$

8. Analytical aspects of linearized stability

In this section, we consider the systems of equations (7.7) and (7.8) and linearize them about a steady flow, assuming that the perturbations have the form used in linearized stability calculations. Thus let V stand for any of the variables $(F, G, W_{11}, \ldots, W_{30})$ and let

$$V(z, t, \epsilon) = V^0(z) + \epsilon\, \mathrm{e}^{\sigma t} v(z) + O(\epsilon^2), \tag{8.1}$$

where V^0 denotes the steady-state value and v the perturbation term. Letting $(w_1, w_2, w_3, \ldots, w_8)$ stand for the perturbations in the variables $(F, G, W_{11}, \ldots, W_{30})$ respectively and expanding (7.7) and (7.8) to the first order in ϵ, the result is:

$$\left.\begin{aligned}
\sigma R w_1'' &= \beta w_1^{\mathrm{iv}} + 3w_3' - w_6' + w_5'' \\
&\quad + 2R[F^0 w_1''' + F^{0'''} w_1 + G^0 w_2' + G^{0'} w_2], \\
\sigma R w_2 &= \beta w_2'' + 4w_4 + w_7' \\
&\quad + 2R[F^0 w_2' - F^{0'} w_2 + G^{0'} w_1 - G^0 w_1'], \\
\sigma\lambda w_3 &= -w_3 + 2\lambda[F^0 w_3' + W_{11}^{0'} w_1 + F^{0''} w_5 + W_{13}^0 w_1''], \\
\sigma\lambda w_4 &= -w_4 + \lambda[2F^0 w_4' + 2W_{12}^{0'} w_1 \\
&\quad + G^{0'} w_5 + W_{13}^0 w_2' + F^{0''} w_7 + W_{23}^0 w_1''], \\
\sigma\lambda w_5 &= -w_5 + (1-\beta) w_1'' + \lambda[2F^0 w_5' - 2F^{0'} w_5 \\
&\quad + 2W_{13}^{0'} w_1 - 2W_{13}^0 w_1' + F^{0''} w_8 + W_{30}^0 w_1''], \\
\sigma\lambda w_6 &= -w_6 + 2\lambda[F^0 w_6' + W_{22}^{0'} w_1 + G^{0'} w_7 + W_{23}^0 w_2'], \\
\sigma\lambda w_7 &= -w_7 + (1-\beta) w_2' + \lambda[2F^0 w_7' - 2F^{0'} w_7 \\
&\quad + 2W_{23}^{0'} w_1 - 2W_{23}^0 w_1' + G^{0'} w_8 + W_{30}^0 w_2'], \\
\sigma\lambda w_8 &= -w_8 - 4(1-\beta) w_1' \\
&\quad + 2\lambda[F^0 w_8' - 2F^{0'} w_8 + W_{30}^{0'} w_1 - 2W_{30}^0 w_1'].
\end{aligned}\right\} \tag{8.2}$$

The boundary conditions on w_1, w_1' and w_2 are of course given by

$$\left.\begin{aligned}
w_1(0) = 0, \quad w_1(1) = 0, \quad w_2(0) = 0, \\
w_1'(0) = 0, \quad w_1'(1) = 0, \quad w_2(1) = 0.
\end{aligned}\right\} \tag{8.3}$$

Thus (8.2) constitutes an eigenvalue problem for σ of the form

$$\boldsymbol{A}\boldsymbol{w} = \sigma \boldsymbol{B}\boldsymbol{w}. \tag{8.4}$$

We now derive the basic equation that governs the linearized stability of the torsional flow. Put $R = 0$ in (8.2), use the velocity field (4.2) of the torsional flow so that

$$F^0(z) = 0, \quad G^0(z) = 1 + (\gamma - 1) z, \tag{8.5}$$

and use (7.9) to find that

$$\left.\begin{aligned}
W_{11}^0 &= W_{12}^0 = W_{13}^0 = W_{30}^0 = 0, \\
W_{22}^0 &= 2\lambda(1-\beta)(\gamma-1)^2, \\
W_{23}^0 &= (1-\beta)(\gamma-1).
\end{aligned}\right\} \tag{8.6}$$

Then the system (8.2) leads to the eigenvalue problem

$$w_1^{\mathrm{iv}} + 4\xi^2 w_1'' = 0, \tag{8.7}$$

where the parameter ξ is given by

$$\xi^2 = \frac{\lambda^2(1-\beta)(\gamma-1)^2[3 + 2(1-\beta) + \lambda\sigma(4+\lambda\sigma)]}{(1+\lambda\sigma)^2(1+\lambda\beta\sigma)^2}. \tag{8.8}$$

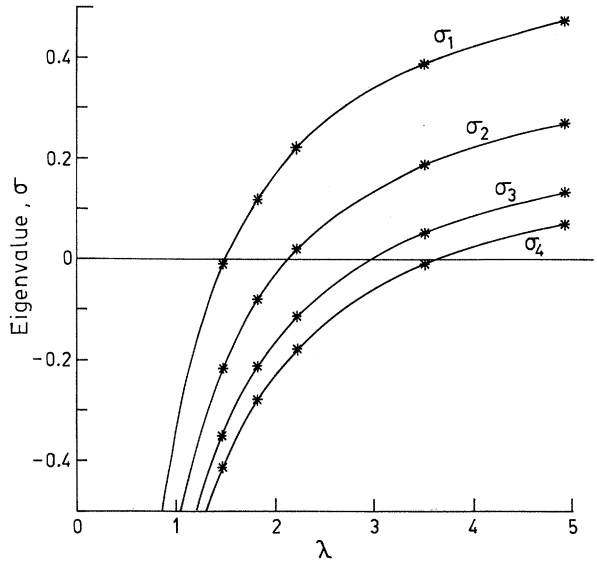

Figure 16. The first four eigenvalues for the stability of the torsional flow. σ as a function of λ, while keeping $R = 0$, $\beta = 0.5$, $\gamma = -0.5$ fixed. See (8.11).

Setting $\sigma = 0$ in (8.8), we recover (5.13) as we should. Again, it follows that (8.7) has non-trivial solutions only if

$$\left.\begin{aligned} \xi &= n\pi, \quad n = 1, 2, \ldots \\ \xi &= \tan \xi. \end{aligned}\right\} \tag{8.9}$$

The smallest root of (8.9) is $\xi = \pi$. Using this in (8.8) and putting $\sigma = 0$, one recovers the result of Phan-Thien (1983*b*) that the torsional flow is unstable if

$$\pi^2 = \lambda^2(1-\beta)\,(\gamma-1)^2[3+2(1-\beta)]. \tag{8.10}$$

Of course, this result is to be expected because (8.4) is a linear eigenvalue problem for σ, and when this parameter is zero, (8.4) is equivalent to seeking bifurcations from the steady torsional flow and this is why (5.13) and (8.8) lead to identical results.

Now in order to compare the theoretical results with their numerical counterparts, consider the case when $\beta = 0.5$, $\gamma = -0.5$. Then, for each value of ξ, (8.8) gives the relation

$$\sigma(\lambda) = \tfrac{3}{\sqrt{2}}\,1/\xi - 1/\lambda. \tag{8.11}$$

Our numerical calculations have verified that the formula (8.11) represents the crossing of a single real eigenvalue of (8.2) from the negative to the positive real axis. Thus, in the case when $\beta = 0.5$, $\gamma = -0.5$, $R = 0$, as λ is increased from 0, the torsional flow is stable up to $\lambda_1 = 1.481$ and unstable beyond that. At each successive value of λ obtained from the relation

$$\lambda_i = \tfrac{\sqrt{2}}{3}\,\xi_i, \tag{8.12}$$

another eigenvalue σ_i crosses to the positive real axis and remains positive for all $\lambda > \lambda_i$, being asymptotic to

$$\sigma_i = 1/\lambda_i. \tag{8.13}$$

This is depicted in figure 16.

9. A numerical examination of stability of axisymmetric flows

The system (8.2)–(8.3) was discretized on the same mesh that was used for the steady-state calculations in §6. That is, we divide the interval $[-\frac{1}{2}\Delta z,\ 1+\frac{1}{2}\Delta z]$ into J subintervals, where $\Delta z = 1/(J-1)$. The finite difference approximations used at the interior mesh points $2 \leqslant j \leqslant J-2$ for any variable V are given by (cf. (6.5)–(6.7)):

$$\left.\begin{aligned} V_j &= V(z_j), \\ V_j' &= (V_{j+1}-V_{j-1})/2\Delta z, \\ V_j'' &= (V_{j+1}-2V_j+V_{j-1})/\Delta z^2, \\ V_j''' &= (V_{j+2}-2V_{j+1}+2V_{j-1}-V_{j-2})/2\Delta z^3, \\ V_j^{\mathrm{iv}} &= (V_{j+2}-4V_{j+1}+6V_j-4V_{j-1}+V_{j-2})/\Delta z^4. \end{aligned}\right\} \tag{9.1}$$

At the boundaries, we have (for $j = 0,\ 1,\ J-1,\ J$):

$$\left.\begin{aligned} V(0) &= \tfrac{1}{2}(V_1+V_0), \qquad V(1) = \tfrac{1}{2}(V_J+V_{J-1}), \\ V'(0) &= (V_1-V_0)/\Delta z, \quad V'(1) = (V_J-V_{J-1})/\Delta z. \end{aligned}\right\} \tag{9.2}$$

The above formulae are all *central* difference formulae, accurate to $O(\Delta z^2)$. Note that the derivatives V''' and V^{iv} are not required at the mesh points $0, 1, J-1, J$ where the boundary conditions for w_1 and w_1' are implemented. This can be seen in the construction of the matrices $\boldsymbol{A}$ and $\boldsymbol{B}$ below.

Now, as stated in (7.5) we have converted the system of constitutive equations from that relevant to the stresses $\boldsymbol{S}$ to that valid for $\boldsymbol{W}$. A glance at (7.9) shows that we need F'' and G' at the end points $z = 0$ and $z = 1$. Since (9.2) cannot provide the values of $F''(0)$ and $F''(1)$ we use the *forward* difference $O(\Delta z)$-approximation instead. That is, we write

$$\left.\begin{aligned} F''(0) &= (F_2-2F_1+F_0)/\Delta z^2 \\ F''(1) &= (F_J-2F_{J-1}+F_{J-2})/\Delta z^2. \end{aligned}\right\} \tag{9.3}$$

Although this results in a slight loss of accuracy, the scheme was found to work well in providing the eigenvalues, except close to singular points where the eigenvalues become small. An alternative approach using a consistently second-order scheme as in §6, would have resulted in a very complicated form for the matrix $\boldsymbol{B}$ of (8.4) under discretization. The success of our method made it unnecessary to investigate this approach, a conclusion also reached by Walsh (1986) in his thesis.

We shall now describe the construction of the discretized version of the matrix $\boldsymbol{B}$. Symbolically, the operator $\boldsymbol{B}$ can be written as (cf. (8.2)–(8.4)):

$$\boldsymbol{B} = \mathrm{diag}\,[R\mathrm{d}^2/\mathrm{d}z^2, R, \lambda, \ldots, \lambda], \tag{9.4}$$

which has this simple diagonal form because of the choice of variable in (7.5). Next, let the number of intervals $J = 25$. Then define a $(J+1)\times(J+1)$ matrix D_2 through

$$D_2 = \begin{pmatrix} 1 & 1 & 0 & . & . & . & . & 0 \\ 1 & -1 & 0 & . & . & . & . & 0 \\ 0 & 1 & -2 & 1 & 0 & . & . & 0 \\ . & . & . & . & . & . & . & . \\ . & . & . & . & . & . & . & . \\ 0 & . & . & 0 & 1 & -2 & 1 & 0 \\ 0 & . & . & . & . & 0 & 1 & -1 \\ 0 & . & . & . & . & 0 & 1 & 1 \end{pmatrix}. \tag{9.5}$$

Clearly, the matrix D_2 takes care of the boundary values of w_1 and its derivative w_1' as well as the derivative w_1'' in the interior. Next, define a second $(J+1)\times(J+1)$ matrix M through

$$M = \begin{pmatrix} 1 & 1 & 0 & \cdot & \cdot & \cdot & \cdot & 0 \\ 0 & 1 & 0 & \cdot & \cdot & \cdot & \cdot & 0 \\ 0 & 0 & 1 & \cdot & \cdot & \cdot & \cdot & 0 \\ \cdot & \cdot & \cdot & \cdot & \cdot & \cdot & \cdot & \cdot \\ \cdot & \cdot & \cdot & \cdot & \cdot & \cdot & \cdot & \cdot \\ 0 & \cdot & \cdot & \cdot & \cdot & 1 & 0 & 0 \\ 0 & \cdot & \cdot & \cdot & \cdot & \cdot & 1 & 0 \\ 0 & \cdot & \cdot & \cdot & \cdot & \cdot & 1 & 1 \end{pmatrix}. \tag{9.6}$$

This matrix is to take care of the boundary values of w_2 and its interior representation. Finally, let I_n denote the $n\times n$ identity matrix. Hence the matrix $\boldsymbol{B}$ is an $8(J+1)\times 8(J+1)$ matrix of the form

$$\boldsymbol{B} = \operatorname{diag}[RD_2, RM, \lambda I_{6(J+1)}]. \tag{9.7}$$

Similar to $\boldsymbol{B}$ is the $8(J+1)\times 8(J+1)$ discretized form of $\boldsymbol{A}$ corresponding to the right side of (8.2). Here, the rows 1, 2, J, $J+1$, $J+2$ and $2(J+1)$ of $\boldsymbol{A}$ are zero to incorporate the boundary conditions on w_1 and w_2. This means that six eigenvalues of the discretized problem will always be zero.

Now it is fairly easy to assemble the matrix form of $\boldsymbol{A}$ and the only point to remember is that rows corresponding to the exterior mesh points 0 and J for the constitutive equations contain the equations at $z=0$ and $z=1$, not at $z=-\frac{1}{2}\Delta z$, $z=1+\frac{1}{2}\Delta z$.

Having assembled the matrices $\boldsymbol{A}$ and $\boldsymbol{B}$, the eigenvalues of $\boldsymbol{B}^{-1}\boldsymbol{A}$ were computed using a standard NAGLIB routine. Now, if λ or R is zero, then $\boldsymbol{B}$ becomes singular and the eigenvalue problem must be reformulated to accommodate these cases. Although this is not difficult to do and indeed has been done by Walsh (1986) for $R=0$, it is much easier to simply put λ or R off zero by a very small amount (say 10^{-4} using the pseudo-arc-length continuation method). Since the eigenvalues vary continuously with these two parameters their change is also very small when the parameters increase from zero. This method thus provided an entirely adequate treatment of the singular cases within the above scheme.

To illustrate the results from the calculations, which generally take about ten minutes per problem, we consider the Example Set I from §6. Keeping the values of $R=0$, $\beta=0.5$, $\gamma=-0.5$ fixed, the calculated points in the (σ,λ) plane have been compared with the theoretical curves arising from the equation (8.11). The results are depicted in figure 16 above.

Next in the above example, we keep the parameters β and γ fixed and, using pseudo-arc-length continuation, calculate the solution surfaces for $R=0$ and $R\approx 0.1$ with varying λ. The curves in figure 17 are obtained, showing a complicated structure of bifurcations and folds; in connection with the folds, see figure 6 for their location. The dotted lines in figure 17 represent expected extrapolations into regions where the numerical method developed convergence problems. We now give a description of the various branches.

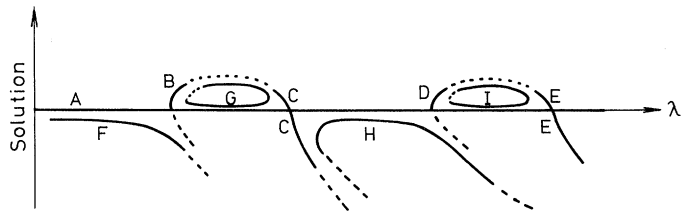

Figure 17. Solution surfaces with varying λ, for $R = 0$ and $R \approx 0.1$. Here $\beta = 0.5$ and $\gamma = -0.5$ are fixed.

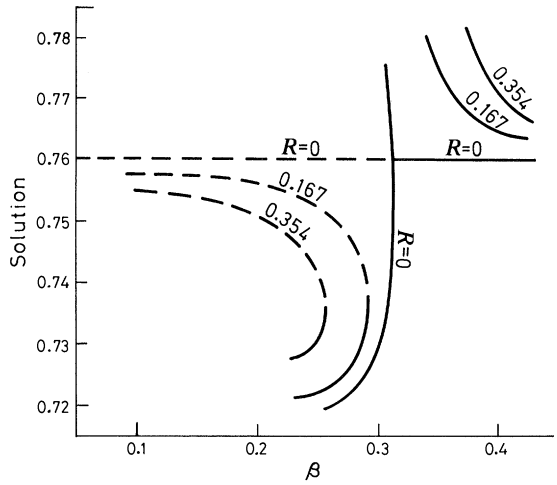

Figure 18. Stability of solutions with $\gamma = 0.5$, $\lambda = 3.6$ fixed while R and β are varied. See figures 8 and 9 in connection with this.

$R = 0$: Branches A, B, C, D, E.

$R \approx 0.1$: Branches F, G, H, I.

Branch A is the torsional flow and is valid for all $\lambda > 0$. The flow is stable up to the first bifurcation point at $\lambda = 1.481$, then becomes unstable acquiring a further positive eigenvalue with each bifurcation point crossing on the λ axis. See figure 16 in connection with this.

Branch F was found to be stable, as expected by R-continuation from A in this region. All other branches B, C, D, E, G, H and I were found to be unstable. Each of these showed positive eigenvalues σ which could be identified as the continuation (in R or λ) of the (positive) eigenvalues $\sigma_1(\lambda)$ and $\sigma_2(\lambda)$ belonging to the torsional flow branch A.

The next figure 18 illustrates the solution surfaces associated with the Example Set II. Keeping $\gamma = 0.5$ and $\lambda = 3.6$ fixed, we have constructed the curves of $w_2(z)$ against β at the mesh point nearest to $z = 0.5$. Denoting by the dashed curve, the unstable solution and by the continuous curve the stable one, it is found that the simple bifurcation point for $R = 0$ at $\beta = 0.311$ is seen to develop into a fold as R increases. See figure 10 in this connection where the position of the limit point in the $R\beta$-plane is depicted. It is found that an exchange of stability occurs at the limit point.

PART B. NON-AXISYMMETRIC MOTIONS

In this part, we begin in §10 with the equations that govern the non-axisymmetric, *steady* flows of the Oldroyd-B fluid in the two-disc configuration. After discussing the kinematics (Parter & Rajagopal 1984; Huilgol & Rajagopal 1987) we list the constitutive equations satisfied by the stress functions (Huilgol & Rajagopal 1987), the modified stress functions obtained by using the transformations listed above in §3 and the equations of motion in terms of the latter. In addition, some alterations are also made to the modified stress functions due to a change in the boundary conditions to make the latter independent of the parameter α, which is a measure of the non-axisymmetry. Full details are available in the Appendix.

In §11, we provide the numerical results obtained by combining the results of §5, §6 and §10. Thus, we are able to exhibit many examples of the non-axisymmetric flows of the Oldroyd-B fluid in the two-disc configuration. The physical significance of the non-axisymmetric flows lies in their importance in torsional flow rheometers where they will arise due to a misalignment of the two discs.

10. Steady non-axisymmetric flows

Let $(\hat{x}, \hat{y}, \hat{z})$ denote the cartesian coordinates and let these be non-dimensionalized through (cf. (3.1)):

$$\hat{x} = xd, \quad \hat{y} = yd, \quad \hat{z} = zd. \tag{10.1}$$

Let the velocity field $\hat{\boldsymbol{v}}$ be scaled as in (2.3), i.e.

$$\hat{\boldsymbol{v}} = \boldsymbol{\Omega}_0 \boldsymbol{v}, \tag{10.2}$$

where $\boldsymbol{\Omega}_0$ denotes the steady, angular velocity of the bottom disc situated at $z = 0$. Now, let (u, v, w) denote the velocity components of the field $\boldsymbol{v}$ such that (cf. Parter & Rajagopal 1984; Huilgol & Rajagopal 1987):

$$\left.\begin{aligned} u &= xF' - yG + \alpha g, \\ v &= xG + yF' - \alpha f, \\ w &= -2F, \end{aligned}\right\} \tag{10.3}$$

where F, G, f, and g are all functions of the coordinate z, and the prime denotes differentiation with respect to z. The functions F, G are the axisymmetric components, whereas f, g are the non-axisymmetric ones. The boundary conditions are the same as (3.3) for the functions F, G, while the new functions f, g are required to meet:

$$\left.\begin{aligned} f(0) &= 0, \quad g(0) = 0, \\ f(\tfrac{1}{2}) &= 1, \quad g(\tfrac{1}{2}) = 0, \\ f(1) &= 0, \quad g(1) = 0. \end{aligned}\right\} \tag{10.4}$$

In (10.4), the boundary conditions on $z = 0$ and $z = 1$ follow from the adherence conditions, whereas on the plane $z = \frac{1}{2}$ a measure of non-axisymmetry has been introduced through $f(\frac{1}{2})$. In fact, it is easily seen from (10.3) that on the plane $z = \frac{1}{2}$ as $(x, y) \to (0, 0)$, the in-plane components $(u, v) \to (0, -\alpha)$. Hence, the non-axisymmetric equations depend on the parameter α and thus we have a one-parameter problem and in order to emphasize this, the constant α has been included in (10.3).

Now, let the velocity field (10.3) be substituted into the constitutive equation (2.4). It is found that the stress tensor $\boldsymbol{S}$ is a quadratic in x and y, with coefficients

that are functions of z. Indeed, the components of $\boldsymbol{S}$, denoted by $S\langle ij\rangle$, have the following representation (Huilgol & Rajagopal 1987)

$$\left.\begin{aligned} S\langle ij\rangle &= \sum_{k+m=0}^{2} \tilde{S}_{ijkm}\, x^k y^m, \quad i,j = 1,2, \\ S\langle ij\rangle &= \sum_{k+m=0}^{1} \tilde{S}_{ijkm}\, x^k y^m, \quad i = 1,2; j = 3, \\ S\langle 33\rangle &= \tilde{S}_{3300}. \end{aligned}\right\} \tag{10.5}$$

There are, in fact, twenty five stress functions in (10.5). The reader's attention is directed to the Appendix for a discussion of the equations satisfied by $\tilde{S}_{ijkm}$ and the modified functions T_{ijkm}.

The equations of motion for the velocity field (10.1) can be derived quite easily when use is made of the representation of the stresses in (10.5). One obtains (Huilgol & Rajagopal 1987):

$$\left.\begin{aligned} 2\tilde{S}'_{1120} + \tilde{S}'_{1121} + \tilde{S}''_{1310} &= -2R(FF''' + GG'), \\ \tilde{S}_{1111} + 2\tilde{S}_{1202} + \tilde{S}'_{1301} &= 2R(FG' - F'G), \\ \tilde{S}'_{1110} + \tilde{S}'_{1201} + \tilde{S}''_{1300} &= R\alpha(f'G + fG' + F''g - F'g' - 2Fg''), \\ \tilde{S}'_{1210} + \tilde{S}'_{2201} + \tilde{S}''_{2300} &= R\alpha(2f''F + f'F' - fF'' + gG' + g'G). \end{aligned}\right\} \tag{10.6}$$

As shown clearly by Huilgol & Rajagopal (1987), the first two of the above equations are the axisymmetric flow equations (3.7) and (3.9) in the new coordinate system, and hence they determine the functions F, G. The next two are to be used to find the new functions f, g. The reader's attention is drawn once again to the Appendix, where the conversion of (10.6) to a system which is easier for computational purposes has been made. Thus we arrive at the following eight equations:

$$\left.\begin{aligned} &T_{1110} + \lambda[2gT_{11} + 2fT_{12} - 2g'T_{13} - F'T_{1110} + GT_{2201} - 2F''T_{1300} \\ &\qquad - 2FT'_{1110} + 4(1-\beta)\,(\lambda(gF'' + fG')\,F'' - g'F'')] = 0, \\ &T_{1101} + \lambda[2g'T_{23} - 2gT_{12} - 2fT_{22} - F'T_{1101} - GT_{2210} + 2G'T_{1300} \\ &\qquad - 2FT'_{1101} + 4(1-\beta)\,(g'G' - \lambda(gF'' + fG')\,G')] = 0, \\ &T_{2210} + \lambda[2gT_{22} - 2fT_{12} + 2f'T_{23} - F'T_{2210} + GT_{1101} - 2G'T_{2300} \\ &\qquad - 2FT'_{2210} + 4(1-\beta)\,(\lambda(gG' - fF'')\,G' + f'G')] = 0, \\ &T_{2201} + \lambda[2gT_{12} - 2fT_{11} + 2f'T_{13} - F'T_{2201} - GT_{1110} - 2F''T_{2300} \\ &\qquad - 2FT'_{2201} + 4(1-\beta)\,(\lambda(gG' - fF'')\,F'' + f'F'')] = 0, \\ &T_{1300} + \lambda[gT_{13} + fT_{23} - g'T_{30} + F'T_{1300} + GT_{2300} - 2FT'_{1300} \\ &\qquad + (1-\beta)\,(5g'F' + gF'' - 2g''F + fG' - f'G)] = 0, \\ &T_{2300} + \lambda[gT_{23} - fT_{13} + f'T_{30} + F'T_{2300} - GT_{1300} - 2FT'_{2300} \\ &\qquad + (1-\beta)\,(gG' - g'G + 2f''F - fF'' - 5f'F')] = 0, \\ &3T'_{1110} - T'_{2210} + 2T''_{1300} + 2g''' = 2R(gF'''' + f'G + fG' - 2g''F - g'F'), \\ &3T'_{2201} - T'_{1101} + 2T''_{2300} - 2f''' = 2R(g'G + gG' - fF'' + 2f''F + f'F'). \end{aligned}\right\} \tag{10.7}$$

What the above system tells us is that, given the functions F, G, $T_{11}, \ldots, T_{30}$, the functions f, g, $T_{1110}, \ldots, T_{2300}$ are uniquely determined because (10.7) is linear. Hence for every axisymmetric flow, given the non-axisymmetry parameter α in the centre plane, there is a unique non-axisymmetric flow.

As an example, we now list from Huilgol & Rajagopal (1987) the analytical solution to the system (10.7) when the underlying axisymmetric flow system is the rigid body motion. They introduced the following new function (Berker 1979; Huilgol & Rajagopal 1987):

$$N(z) = f(z) + \mathrm{i}g(z), \tag{10.8}$$

where $\mathrm{i}^2 = -1$, and showed that $N(z)$ must satisfy

$$N''' = \mathrm{i}R(1-\mathrm{i}\lambda)N'/(1-\mathrm{i}\lambda\beta). \tag{10.9}$$

The above third order equation has the following solution:

$$N(z) = A_0 + A_1 \mathrm{e}^{\mu_1 z} + A_2 \mathrm{e}^{\mu_2 z}, \tag{10.10}$$

where μ_1, μ_2 are the two roots of

$$\mu^2 = \mathrm{i}R(1-\mathrm{i}\lambda)/(1-\mathrm{i}\lambda\beta). \tag{10.11}$$

The three constants A_0, A_1, A_2 in (10.10) are found quite easily from the conditions (10.4) on f and g. Although we have decided not to draw the functions f and g, it is clear that they possess a complicated structure.

Next, for a newtonian fluid, if the basic flow is the torsional flow, the non-axisymmetric flow components are easily obtained. Putting $\lambda = 0$, $R = 0$ in (10.7) one finds that

$$f(z) = 4z(1-z), \quad g(z) = 0. \tag{10.12}$$

On the other hand, despite numerous attempts, it has not been possible to obtain an analytic solution to the equations which describe the non-axisymmetric components in the Oldroyd-B fluid arising from a basic flow which is the torsional flow. Given this situation, for more general basic flows, it is obvious that the only way to solve the system (10.7) is through numerical means and we exhibit some examples in §11.

11. A numerical study of non-axisymmetric flows

As stated in the previous §10, there is a unique non-axisymmetric flow for every axisymmetric flow and, in this section, we choose some axisymmetric flows and find the non-axisymmetric flow components $\Delta f, g$ that correspond to the former. Here, Δf is the excess of f over the newtonian torsional flow contribution (10.12), i.e.

$$\Delta f(z) = f(z) - 4z(1-z). \tag{11.1}$$

Although it is possible to generate many solutions a restriction arises from the fact that the system may become stiff due to the coefficients, which depend on the axisymmetric flow components, becoming very large. Hence, we do not include the problematic cases, only showing the relatively easy solutions.

(a) *Example Set I*

The first set consists of those flows with $\beta = 0.5$, $\gamma = -0.5$. Hence these non-axisymmetric flows correspond to those in the Example Set I in §6. We depict two specific situations:

(i) If the basic flow is the torsional flow and $R = 0$ is kept fixed, then a bifurcation occurs at $\lambda = 1.481$. If we use regular continuation until $\lambda = 2.0$ is reached, then the functions Δf and g have the forms shown in figure 19. Note that neither Δf nor g is symmetric about the centreline although F and ΔG are (see figure 2).

(ii) If we keep $\lambda = 2.0$ fixed and vary R from zero to 0.24, then figure 20 results. Again the non-axisymmetric flow parts are not symmetric.

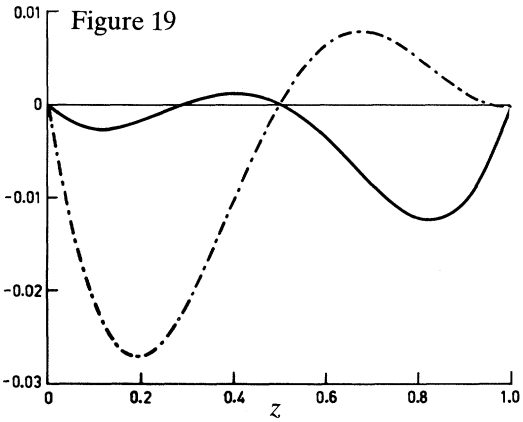

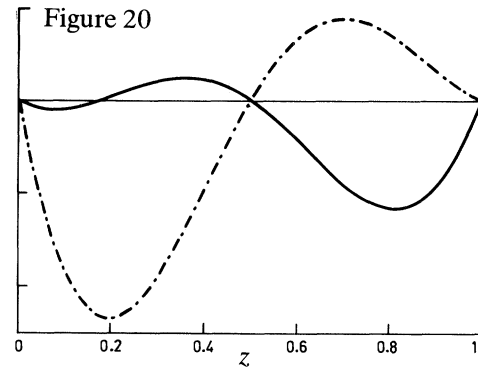

Figure 19. Solution on bifurcation branch obtained from figure 2 with $R = 4.3 \times 10^{-13}$, $\lambda = 2.0$. ——, g; – – –, Δf.

Figure 20. Solution at limit point in figure 3 with $R = 0.24$ and $\lambda = 2.0$. ——, g; – – –, Δf.

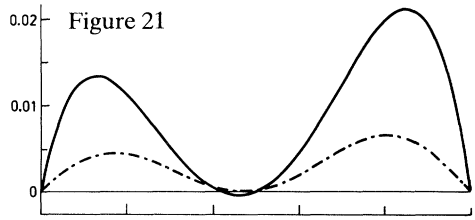

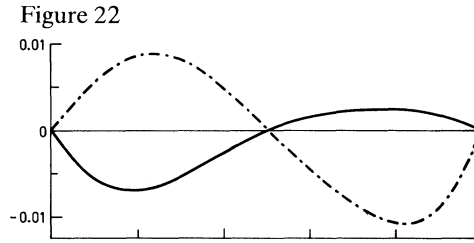

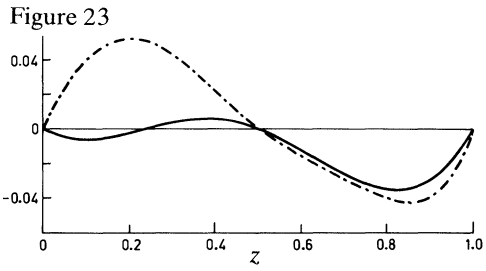

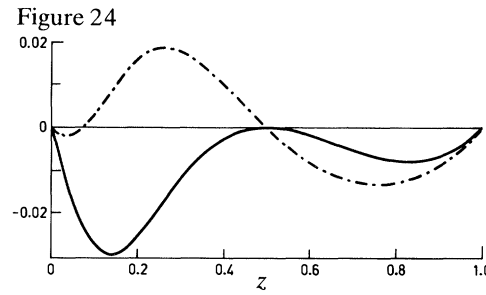

Figures 21–24. ——, g; – – –, Δf.

Figure 21. Flow corresponding to that in figure 7 when $R = 50$ and $\beta = 0.98$, the almost newtonian fluid.

Figure 22. Flow corresponding to that in figure 8 when $R = 0.73$ and $\beta = 0$, the Maxwell fluid.

Figure 23. Flow associated with the limit point flow in figure 9 when $R = 0.1$ and $\beta = 0.3$.

Figure 24. Flow at the first limit point arising from figure 14 with $\gamma = -0.0055$, $\lambda = 0.05$.

(*b*) *Example Set II*

Here there are three examples with $\gamma = -0.5$ and $\lambda = 3.6$ fixed and thus we are dealing with the situations corresponding to the Example Set II in §6. From the Maxwell fluid ($\beta = 0$) to the almost newtonian fluid ($\beta = 0.98$) the patterns of Δf and g change as can be seen in figures 21–23.

PHILOSOPHICAL TRANSACTIONS OF THE ROYAL SOCIETY A MATHEMATICAL, PHYSICAL & ENGINEERING SCIENCES

(c) *Example Set VI*

Here, corresponding to that in figure 14 of the Example Set VI in §6 is the figure 24.

In summary, it can be seen that the non-axisymmetric flow components are not symmetric about the centreline $z = 0.5$ even if the axisymmetric parts are. In this connection, see figures 25 and 26 below as well.

12. Concluding remarks

The present work has explored in detail the solutions that arise in the coaxial disc problem for the Oldroyd-B fluid. First and foremost, the use of a robust numerical scheme, capable of dealing with regular and limit point bifurcations, has shown that the high Weissenberg problem is not a real one. That is to say, we have been able to generate solutions for values of the parameter λ as high as 4.0. Hence previous difficulties in dealing with high values of this parameter are consequences of the numerical schemes used therein. For example, $\gamma_w = -0.5$ used by Walsh (1987) corresponds to $\gamma = -1$ here and from (6.1) we see that this means a relaxation time $\tilde{\lambda} = 0.15$ which is far less than 4.0. We note that Ji *et al.* (1990) have also achieved a numerical value of 4.0 in their work. Similarly, the values of $W = 1.4$, $\gamma_w = 1$ correspond respectively to $\lambda = 1.4$, $\gamma = 2$. The results for the latter can be read off, on account of the *Scaling Lemma*, from those for the set $(\tilde{\lambda}, \tilde{\gamma}) = (2.8, 0.5)$. In sum, the range of relaxation parameter values achieved here surpasses those in the work of Walsh (1986, 1987).

We now comment on the figures 2–5. The effect of increasing the relaxation time λ can be seen in connection with the torsional flow when $R = 0$. This flow remains symmetric about $z = 0.5$ till λ reaches 2.0 (see figure 2). Comparing these curves with those in fig. 2*b* and *c* of Walsh (1987), we see that the effect of increasing the retardation time from $\beta = 0$ (or $\beta_w = 1$) to $\beta = 0.5$ is to reduce the deviation from the torsional flow.

After that as R is increased to 0.24, the symmetry is broken (see figure 3). More striking are the flow curves in figures 4 and 5 which show the results of varying both λ and R. Our results here are similar to those obtained by Ji *et al.* (1990) in their figures 3–5.

The last part of figure 6 shows in detail the way folds appear and disappear in the $R\lambda$-plane as R is increased from 0 to 2.0, while λ goes from 1.2 (before any bifurcation occurs) to 4, passing through four bifurcations in the process. The attention of the reader is also drawn to the figure 17 which shows the stable and unstable branches associated with the above set of flows.

The next set of figures 7–10 demonstrate the combined effects of varying both R and β, with figure 18 depicting the stability of the related flows. The other figures 11–15 are self-explanatory in the details they reveal about the solution surfaces associated with the Oldroyd-B fluid.

In figures 19–24, we have drawn the non-axisymmetric flow components arising from the set of axisymmetric flows. Again, there is a wide variety of possible flow situations.

In conclusion, one can say that the relaxation and the retardation parameters cause the flow to deviate from the torsional flow. The deviation, however, is not significantly large on primary branches. On secondary branches or those reached

PHILOSOPHICAL TRANSACTIONS OF THE ROYAL SOCIETY A MATHEMATICAL, PHYSICAL & ENGINEERING SCIENCES

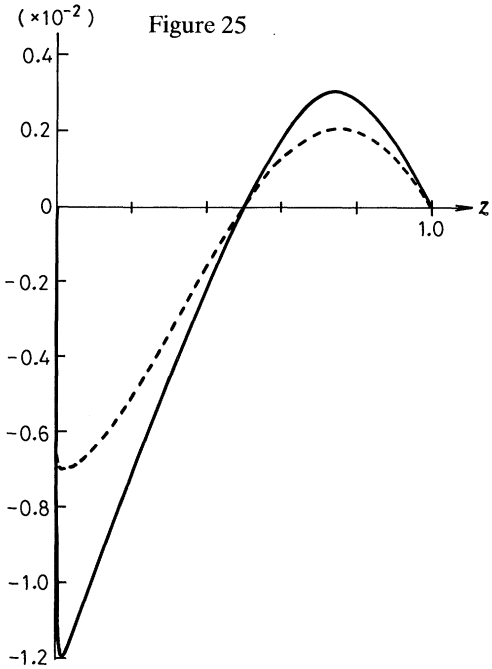

Figure 25

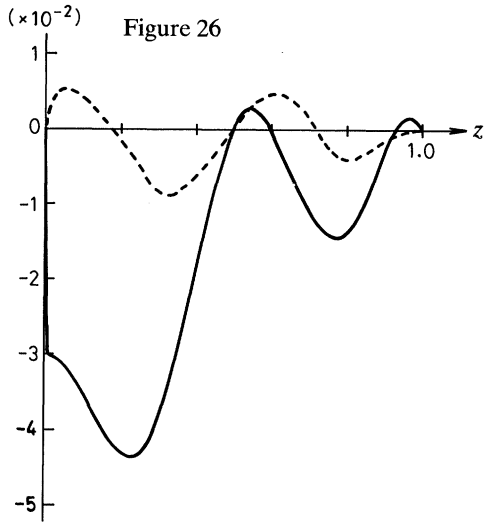

Figure 26

Figure 25. Slip-layer associated with the torsional flow with $R = 0$, $\beta = 0.1$, $\gamma = 2$ and $\lambda = 2.054$.

Figure 26. Slip-layer associated with the secondary branch from the torsional flow for the same values of the four parameters R, β, γ, λ.

from a different sheet (cf. figure 14), the deviation can be considerable. This is also the opinion expressed by Ji *et al.* (1990).

The situation with respect to non-axisymmetric flows is rather different. Relatively large differences from the newtonian non-axisymmetric flow components occur quite readily as may be seen from figures 19–24.

We shall now turn to a comparison with the experimental results of Sirivat *et al.* (1988). They found experimentally that in the axisymmetric flows of a non-newtonian fluid, namely a solution of polyacrylamide, deviations from the newtonian velocity field were small; however, they also noticed that narrow regions of high velocity gradients associated with the tangential velocity fields appeared in the polyacrylamide solution. Our theoretical results are in agreement with these observations for, as already stated, deviations from the newtonian velocity field are small on primary branches. Concurrently, an examination of figures 4 and 5 reveals the existence of relatively moderate steep velocity gradients. However, our results from axisymmetric flows do not reveal the existence of slip-layers seen in figures 6*d*, 7*b* and 9 of Sirivat *et al.* (1988). On the other hand, if a small misalignment in the apparatus existed, then it is more than likely that non-axisymmetric flows occurred in the apparatus used by Sirivat *et al.* Then, it may be seen from figs 2 and 3 of Crewther & Huilgol (1988) dealing with non-axisymmetric flow components (reproduced here as figures 25 and 26 respectively) that slip-layers may exist in the flow of an Oldroyd-B fluid in the two-disc configuration.

The research reported here was begun by R. R. H. during his stay at the California Institute of Technology as a Senior Fulbright Fellow in 1983. R. R. H. thanks the Australian–American

Educational Foundation for this award and Professor H. B. Keller, Department of Applied Mathematics, for inviting him to the California Institute of Technology. Thanks are also due to Dr J. M. Fier for sharing his computer program. The work of I.C. and R.J. was funded by the Australian Research Grants Scheme during the years 1987, 1988 and the early part of 1989. We also thank Mrs J. C. Laing for preparing the numerous drawings for publication.

Appendix

Before we begin it is necessary to draw the attention of the reader to the following: we wish to emphasize that the components $\tilde{S}_{ijkl}$ used in the present paper are obtained from the S_{ijkl} listed in (A 15)–(A 25) of the paper by Huilgol & Rajagopal (1987) after making the following adjustments.

(i) Replace η_0 by 1; (ii) replace λ_1 by λ; (iii) replace λ_2 by $\lambda\beta$; (iv) change G to $2G$; (v) change H to $2F$; (vi) change f to αf; (vii) change g to αg.

With these in mind, we proceed.

As remarked in §10, there are 25 stress functions in the non-axisymmetric flow situation when the flow is described in the cartesian coordinates (x, y, z). Of these, 14 stress functions $\tilde{S}_{1120}, \tilde{S}_{1102}, \ldots, \tilde{S}_{3300}$ are determined by the axisymmetric flow functions F and G alone, that is to say, these 14 appear in the axisymmetric flow. The reason there are 14, rather than the six important ones in §3 has to do with the coordinate system that has been chosen. Indeed, it is easy to show by considering the change of coordinates from (x, y, z) to the (r, θ, z) system that the following relations hold between the various stress functions mentioned above:

$$\left.\begin{aligned} &\tilde{S}_{1120} = \tilde{S}_{2202} = S_{11}, && \tilde{S}_{1102} = \tilde{S}_{2220} = S_{22},\\ &\tilde{S}_{1111} = -\tilde{S}_{2211} = -2S_{12}, && \tilde{S}_{1220} = -\tilde{S}_{1202} = S_{12},\\ &\tilde{S}_{1211} = S_{11} - S_{22}, && \tilde{S}_{1310} = \tilde{S}_{2301} = S_{13},\\ &\tilde{S}_{1301} = -\tilde{S}_{2310} = S_{23}, && \tilde{S}_{3300} = S_{30}. \end{aligned}\right\} \tag{A 1}$$

Hence the system in §3 yields the 14 stress functions $\tilde{S}_{1120}, \ldots, \tilde{S}_{3300}$ in (A 1) and there is no reason to calculate them afresh. Now the system of ordinary differential equations satisfied by the remaining 11 stress functions, namely $\tilde{S}_{1110}, \tilde{S}_{1101}, \tilde{S}_{1100}, \tilde{S}_{2210}, \tilde{S}_{2201}, \tilde{S}_{2200}, \tilde{S}_{1210}, \tilde{S}_{1201}, \tilde{S}_{1200}, \tilde{S}_{1300}$ and $\tilde{S}_{2300}$ is required.

It is necessary to modify these stress functions further in order to simplify the task of computing the functions f and g. To this end, observe that the constitutive equations for $\tilde{S}_{1210}$ and $\tilde{S}_{1201}$ are not really needed because

$$\left.\begin{aligned} \tilde{S}_{1210} &= \tfrac{1}{2}(\tilde{S}_{2201} - \tilde{S}_{1101}),\\ \tilde{S}_{1201} &= \tfrac{1}{2}(\tilde{S}_{1110} - \tilde{S}_{2210}). \end{aligned}\right\} \tag{A 2}$$

Hence, only nine out of the 11 stress functions are required. Next, we transform these remaining nine functions through:

$$\left.\begin{aligned} &\tilde{S}_{1110} = \alpha T_{1110}, && \tilde{S}_{1101} = \alpha T_{1101}, && \tilde{S}_{1100} = T_{1100} + 2F',\\ &\tilde{S}_{2210} = \alpha T_{2210}, && \tilde{S}_{2201} = \alpha T_{2201}, && \tilde{S}_{2200} = T_{2200} + 2F'.\\ &\tilde{S}_{1200} = T_{1200}, && \tilde{S}_{1300} = \alpha T_{1300} + \alpha g', && \tilde{S}_{2300} = \alpha T_{2300} - \alpha f'. \end{aligned}\right\} \tag{A 3}$$

In addition to (A 3), we change the functions S_{ij} to the corresponding T_{ij} of (3.5). The result of these transformations is a set of nine constitutive equations for the stress functions $T_{1101}, T_{1110}, T_{1100}, T_{2201}, T_{2210}, T_{2200}, T_{1200}, T_{1300}$, and T_{2300}. It turns out that we do not need all the nine stress functions because three of the functions, namely T_{1100},

T_{1200}, T_{2200} have no role to play in the equations of motion and are determined by the remaining six functions. Thus, we substitute in the constitutive equations the relevant transformations from (A 3) for the six functions $T_{1110}, T_{1101}, T_{2210}, T_{2201}, T_{1300}$ and T_{2300}, replace the functions $S_{11}, S_{12}, \ldots, S_{30}$ by the respective T_{ij} from (3.5) and cancel out the common factor α that appears in all the six equations. The end result, along with the modified equations of motion, comprise eight equations in all and these are listed in (10.7).

References

Batchelor, G. K. 1951 *Q. Jl Mech. appl. Math.* **4**, 29–41.

Berker, R. 1979 *Arch. Mech.* **31**, 265–280.

Cerutti, J. H. 1975 Ph.D. thesis, Department of Mathematics, University of Wisconsin, Madison.

Crewther, I. & Huilgol, R. R. 1988 *Proc. Xth Int. Cong. Rheology, Sydney*, vol. 1, pp. 285–287.

Fier, J. M. 1984 Ph.D. thesis, Department of Applied Mathematics, California Institute of Technology.

Huilgol, R. R. & Keller, H. B. 1985 *J. non-newt. Fluid Mech.* **18**, 101–110.

Huilgol, R. R. & Rajagopal, K. R. 1987 *J. non-newt. Fluid Mech.* **23**, 423–434.

Ji, Z., Rajagopal, K. R. & Szeri, A. Z. 1990 *J. non-newt. Fluid Mech.* **36**, 1–25.

Joseph, D. D. 1990 *Fluid dynamics of viscoelastic liquids*. New York: Springer-Verlag.

Kármán, T. von 1921 *Z. angew. Math. Mech.* **1**, 232–252.

Keller, H. B. 1987 *Lectures on numerical methods in bifurcation problems*. Tata Institute of Fundamental Research Lecture Series, vol. 79. New York: Springer-Verlag.

Lai, C.-Y., Rajagopal, K. R. & Szeri, A. Z. 1984 *J. Fluid Mech.* **146**, 203–225.

Oldroyd, J. G. 1950 *Proc. R. Soc. Lond.* A **200**, 523–541.

Parter, S. V. 1982 In *Theory and applications of singular perturbations* (ed. W. Eckhaus & E. M. de Jager). Lecture Notes in Mathematics, vol. 942, pp. 258–280. Springer-Verlag.

Parter, S. V. & Rajagopal, K. R. 1984 *Arch. ration. Mech. Anal.* **86**, 305–315.

Phan-Thien, N. 1983*a* *J. Fluid Mech.* **128**, 427–442.

Phan-Thien, N. 1983*b* *J. non-newt. Fluid Mech.* **13**, 325–340.

Rajagopal, K. R. 1991 *Theoret. Comp. Fluid Dyn.* (In the press.)

Rivlin, R. S. & Ericksen, J. L. 1955 *J. ration. Mech. Anal.* **4**, 323–425.

Sirivat, A., Rajagopal, K. R. & Szeri, A. Z. 1988 *J. Fluid Mech.* **186**, 243–256.

Szeto, R. K.-H. 1978 Ph.D. thesis, Department of Applied Mathematics, California Institute of Technology.

Tanner, R. I. 1962 *Z. angew. Math. Phys.* **13**, 573–580.

Walsh, W. P. 1986 Ph.D. thesis, Mechanical Engineering Department, University of Sydney.

Walsh, W. P. 1987 *Z. angew. Math. Phys.* **38**, 495–512.

Received 25 October 1990; revised 9 May 1991; accepted 17 May 1991

PHILOSOPHICAL TRANSACTIONS OF THE ROYAL SOCIETY A MATHEMATICAL, PHYSICAL & ENGINEERING SCIENCES